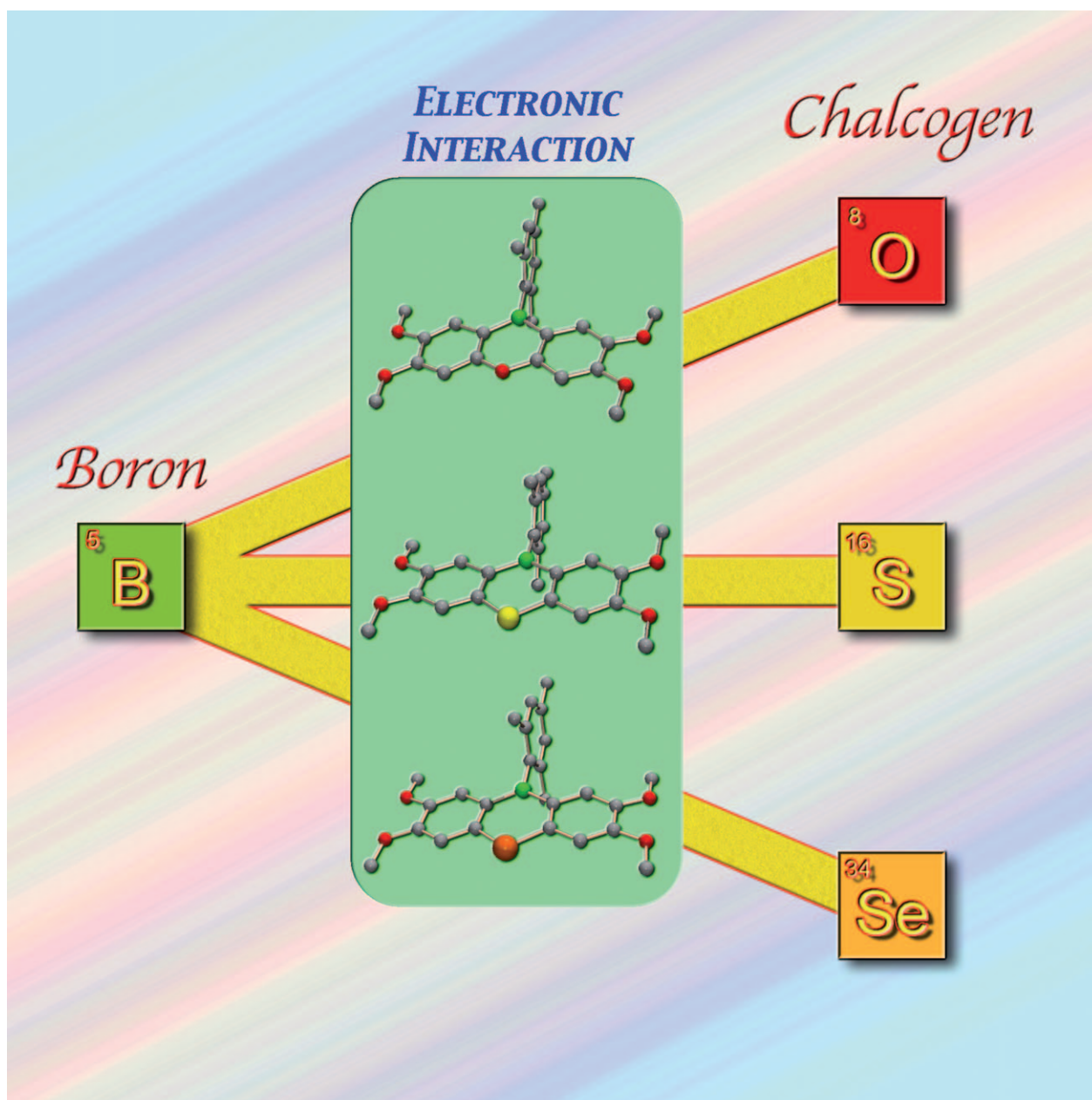# FULL PAPERS

Synthesis of Dibenzochalcogenaborins and Systematic Comparisons of Their Optical Properties by Changing a Bridging Chalcogen Atom

Junji Kobayashi, Keiko Kato, Tomohiro Agou, and Takayuki Kawashima*[a]

Abstract: Novel hetero-π-conjugated compounds (dibenzochalcogenaborins) with the same molecular framework, bearing a boron atom as an acceptor and chalcogen atoms as a donor, were synthesized, and systematic comparisons among these molecules were performed. X-ray crystallographic analysis of these molecules showed similar structures with high planarity. UV/Vis spectroscopy and theoretical calculations revealed that the absorption maxima and the HOMO–LUMO gap cha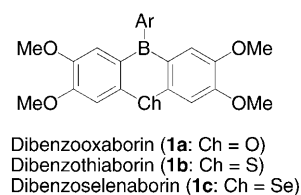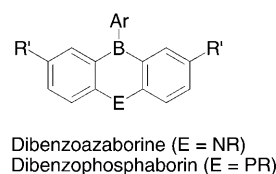nged by systematically changing the bridging chalcogen atom. Dibenzooxaborin and dibenzothiaborin showed fluorescence emission both in solution and in the solid state with a small Stokes shift, indicating the high rigidity of these compounds. On the other hand, dibenzoselenaborin exhibited a very weak fluorescence as a result of the heavy atom effect.

Keywords: conjugation · density functional calculations · fluorescence spectroscopy · heterocycles · UV/Vis spectroscopy

Introduction

π-Conjugated molecules bearing main group elements have attracted much attention in the past decade. Electronic communication between π-orbitals and main group elements can decrease the HOMO–LUMO energy gap by raising the HOMO energy level and/or lowering the LUMO energy level, which leads to excellent photoelectronic properties like photoluminescence. These molecules are utilized as organic light-emitting devices (OLED), organic field-effect transistors (OFET), and so on, in various fields.[1] These properties are strongly influenced by the properties of the main group elements (i.e., electron-donating properties or electron-withdrawing properties, caused by the lone pair, the vacant orbital, or the lower-lying σ* orbital). In other words, change of the main group elements can tune the electronic and optical properties of these molecules. From such a viewpoint, various hetero-π-conjugated molecules containing a main group element, not only electron donors like oxygen, nitrogen, and sulfur, but also electron acceptors like boron, silicon, and phosphorus, have been reported.[2] Among these compounds, boron-containing hetero-π-conjugated molecules are very attractive because their vacant 2p orbital can strongly interact with π-orbitals. Moreover, the vacant 2p orbital is responsive to external stimuli (i.e., Lewis bases). Thus, tricoordinate boron compounds are utilized as optical devices, molecular switches, and molecular sensors.[3]

We have recently focused our interests on dibenzoheteraborins, which are 9,10-dihydroanthracene derivatives containing a boron atom and another main group element. The rigid and planar structures of dibenzoheteraborins are expected to provide synergistic effects between π-orbitals and the boron atom and/or the other bridging main group element. Despite such interesting features, only a few examples of dibenzoheteraborins, (e.g., dibenzoazaborine,[4] dibenzodiborin,[5] dibenzooxaborin,[6] and dibenzothiaborin[7]) have been reported. A detailed study on the optical properties of these compounds was performed only on dibenzoazaborine. Actually, dibenzoazaborines showed acridine-like optical properties with moderately strong fluorescence emission. We have synthesized dibenzophosphaborin,[8] the heavier analog of dibenzoazaborine, and revealed its UV/Vis absorption to be similar to that of dibenzoazaborine, while the photoluminescent properties of dibenzophosphaborin are quite different from those of dibenzoazaborine owing to the structural difference between them. Moreover, the optical properties of dibenzophosphaborin, as well as their reactivity, are varied by a modification on the phosphorus atom. We have also reported the dibenzoazaborines and dibenzothiaborins extend in a ladder-type fashion and showed that their optical properties and reactivity are strongly influenced by the bridging main group elements.[9] From these results, the optical properties and reactivity of dibenzoheteraborins can be tuned by changing the bridging main group element. In the course of our study, we attempt to construct a library

[a] Dr. J. Kobayashi, K. Kato, Dr. T. Agou, Prof. Dr. T. Kawashima
Department of Chemistry, Graduate School of Science
The University of Tokyo
7-3-1 Hongo, Bunkyo-ku, Tokyo 113-0033 (Japan)
Fax: (+81) 3-5800-6899
E-mail: takayuki@chem.s.u-tokyo.ac.jp

Dibenzoazaborine (E = NR)
Dibenzophosphaborin (E = PR)

Dibenzooxaborin (**1a**: Ch = O)
Dibenzothiaborin (**1b**: Ch = S)
Dibenzoselenaborin (**1c**: Ch = Se)

of dibenzoheteraborins with various bridging main group elements.

In this paper we report the synthesis of dibenzochalcogenaborins containing group 16 elements (oxygen, sulfur, and selenium) with the same framework. We also make systematic comparisons on the structures and optical properties of dibenzochalcogenaborins, which can provide information about the influences of bridging main group elements on the optical properties of dibenzoheteraborins.

Results and Discussion

Synthesis

Synthesis of dibenzochalcogenaborins was achieved using a method similar to that of the dibenzoazaborines and dibenzophosphaborins shown in Scheme 1. Dilithiation of bis(2-
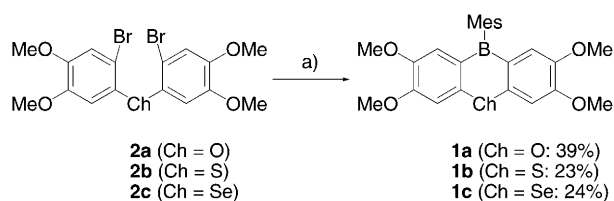
Scheme 1. Synthesis of dibenzochalcogenaborins **1a–1c**. a) i) *t*BuLi (4.4 equiv), −78 °C; ii) MesB(OMe)$_2$ (1.4 equiv), reflux.

bromo-4,5-dimethoxyphenyl) ether **2a**, bis(2-bromo-4,5-dimethoxyphenyl) sulfide **2b**, and bis(2-bromo-4,5-dimethoxyphenyl) selenide **2c**[10] was achieved using 4.4 molar equivalents of *t*BuLi at −78 °C. The generated dilithio derivatives were allowed to react with MesB(OMe)$_2$ to give the desired dibenzochalcogenaborins as pale yellow solids in moderate yields. The dibenzochalcogenaborins are stable in air and moisture. Usually, tricoordinate boron compounds are known to be unstable to oxidation when the steric protection around the boron center is not sufficient and more than two steric protecting groups, the mesityl group for example,

are required to isolate the tricoordinate boron compounds. In the case of dibenzoheteraborins, however, only one mesityl group is enough to protect the boron center as a result of the conformation, in which the mesityl group is almost perpendicular to the chalcogenaborin rings. ^{11}B NMR of dibenzochalcogenaborins **1a–c** showed signals at 52 ppm, 54 ppm, and 57 ppm, respectively. These values are within the typical range of tricoordinate boron compounds. The chemical shifts are slightly shifted up-field on going up the periodic table for the choice of the bridging chalcogen atoms. Such up-field shifts may come from the strength of the electronic donation (**1a** > **1b** > **1c**). This would mean that the difference in electronic donation is not significant since the difference in the chemical shifts are very small.

Structures

Single crystals of **1a–c** were obtained by slow evaporation from saturated solutions of CH$_2$Cl$_2$/MeCN for **1a**, THF for **1b**, and CHCl$_3$/MeOH for **1c**, respectively. ORTEP drawings of **1a–c** are shown in Figure 1. In the cases of **1a** and **1b**, there are two independent molecules in the unit cell, however, only one of them is shown because they have quite similar structures. Their bond lengths and angles are summarized in Table 1. The dibenzochalcogenaborins showed similar structures. The B−C bond lengths in dibenzochalcogenaborin ring of **1a–c** did not show a significant change in spite of varying the bridging chalcogen atom. On the other hand, a slight widening of the C−B−C bond angle and a narrowing of the C−Ch−C angle are observed. The di-

Abstract in Japanese:
アクセプターとしてホウ素原子を、ドナーとして16族元素を有する新規なヘテロπ共役化合物であるジベンゾカルコゲナボリンを合成し、導入した16族元素の及ぼす性質の差違について系統的に検討を行った。X線結晶構造解析の結果、これらはすべて高い平面性を有することが明らかとなった。また紫外可視吸収スペクトル、および理論計算の結果より、HOMO-LUMO ギャップが16族元素の種類によって系統的に変化することが明らかとなった。酸素類縁体と硫黄類縁体では蛍光が観測された。またその Stokes シフトは小さく、化合物の剛直な分子骨格を反映したものであった。一方、セレン類縁体では重原子効果のため、蛍光強度はきわめて弱いものであった。
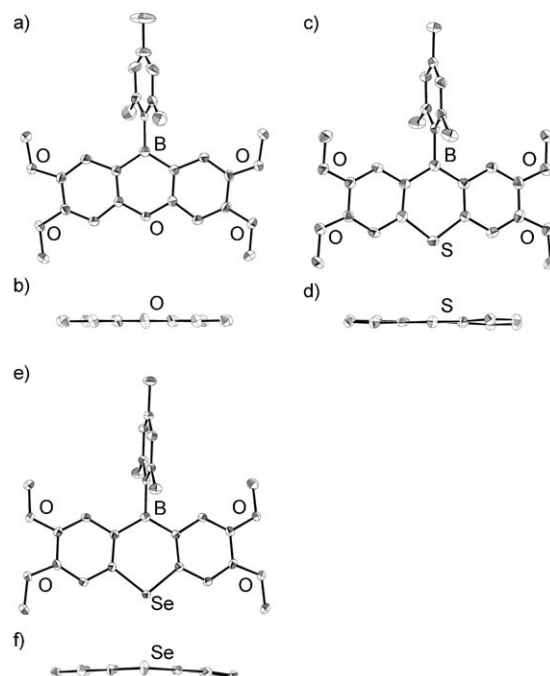
Figure 1. ORTEP drawings of chalcogenaborins **1a–c** (50 % probability). Hydrogen atoms are omitted for clarity. Mesityl and methoxy groups are not shown in side views. a) **1a**, top view. b) **1a**, side view. c) **1b**, top view. d) **1b**, side view. e) **1c**, top view. f) **1c**, side view.

Table 1. Selected bond lengths (Å) and angles (deg) of chalcogenaborins **1a–c**.

	1a[a]	**1b**[b]	**1c**
B−C (in plane)	1.529(2)	1.532(5)	1.550(3)
	1.531(3)	1.537(4)	1.534(4)
	1.530(3)	1.533(5)	
		1.536(4)	
C−Ch	1.366(2)	1.739(3)	1.893(2)
	1.371(2)	1.733(3)	1.888(2)
	1.374(2)	1.743(3)	
		1.746(3)	
C−B−C (in plane)	114.3(2)	119.6(3)	121.4(2)
	114.40(15)	119.7(3)	
C−Ch−C	121.27(19)	106.12(14)	102.05(10)
	121.20(13)	106.32(15)	

[a] Two independent molecules are contained in the unit cell, and one of the molecules has a C_s symmetry. [b] Two independent molecules are contained in the unit cell.

benzochalcogenaborin ring of **1b** is slightly twisted and that of **1c** is slightly puckered. The boron center in **1a–c** takes a completely planar structure. The high planarity found in the dibenzochalcogenaborin rings and around the boron center resulted in the efficient interaction between π-orbitals and molecular orbitals of the boron and chalcogen atoms, leading to good optical properties.

Packing structures of **1a** and **1b** were similar to each other, in which two dibenzochalcogenaborin rings are stacked by a π–π interaction (Figure 2). However, arising
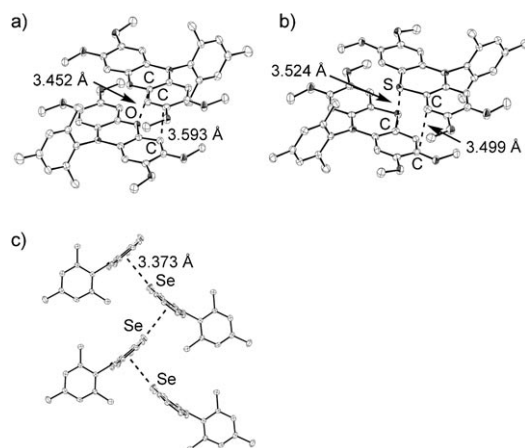

Figure 2. Packing diagram of chalcogenaborins **1a–c** (50% probability). Hydrogen atoms are omitted for clarity. a) **1a**, b) **1b**, c) **1c**, methoxy groups are omitted for clarity. Shortest contacts between two molecules are indicated by dashed lines.

from the bulkiness of the Mes group, the overlap of each dibenzochalcogenaborin ring was small. On the other hand, **1c** had the herringbone packing structure, in which the distance between the selenium atom and the centroid of the fused benzene ring of the neighboring molecule is 3.373 Å, indicating the existence of the interaction between them.

UV/Vis Spectra

UV/Vis spectra of dibenzochalcogenaborins **1a–c** in cyclohexane solution (10^{-4} M) at room temperature are shown in Figure 3 and the data are presented in Table 2. In each spec-
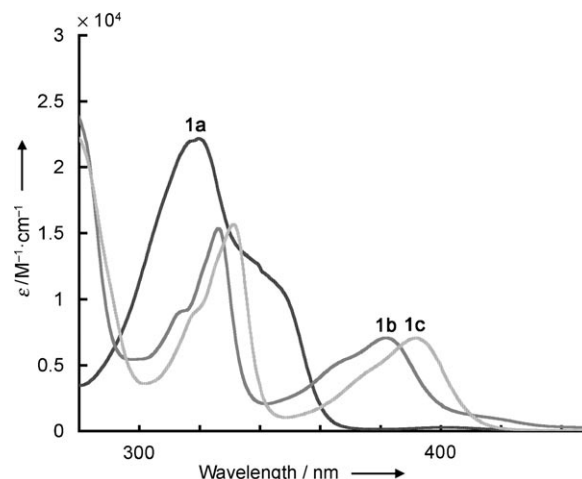

Figure 3. UV/Vis spectra of chalcogenaborins **1a–c** in cyclohexane at 298 K.

Table 2. Optical data for chalcogenaborins **1a–c** in cyclohexane at 298 K.

compound	λ_{max} [nm][a]	ε[b]	λ_{em} [nm][c]	ΔE [cm^{-1}][d]
1a	347(sh)	11 000	377 (0.30)	2.3×10^3
	320	22 000		
1b	382	7100	412 (0.08)	1.9×10^3
	326	15 000		
1c	392	7100	427 (0.0007)	2.1×10^3
	331	16 000		

[a] Absorption maxima in UV/Vis spectra. [b] Absorption coefficient. [c] Emission maxima of fluorescence spectra and quantum yield, determined by using anthracene in cyclohexane as a standard, in parenthesis. [d] $\Delta E = 1/\lambda_{ab} - 1/\lambda_{em}$.

trum, there are two absorption bands. One at 347 nm for **1a**, 382 nm for **1b**, and 392 nm for **1c**, and the other is observed at 320 nm for **1a**, 326 nm for **1b**, and 331 nm for **1c**. The longer wavelength absorptions were attributed to intramolecular charge transfer (ICT) from chalcogen atoms to the boron center and red-shifted on going from **1a** to **1c**. This is because of the smaller HOMO–LUMO gap caused by high energy levels of the chalcogen lone pairs in **1b** and **1c** with heavier chalcogen atoms (vide infra). The shorter wavelength bands are also red-shifted slightly in the order of **1a**, **1b**, and **1c**. These absorption bands are attributed to the transition from HOMO-1 (π-orbital on benzene rings) to LUMO. The energy levels of HOMO-1 of each compound do not change so much (vide infra), and the latter red-shift is attributable to the difference of the LUMO energy levels of each compound.

Fluorescence Spectra

The steady state fluorescence spectra of dibenzochalcogena-borins in cyclohexane solution (10^{-4} M) at room temperature are shown in Figure 4 and the photophysical data are listed
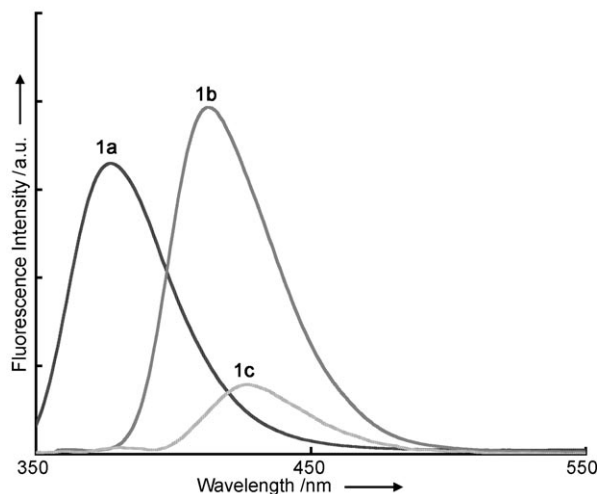

Figure 4. Steady state fluorescence spectra of chalcogenaborins **1a–c** in cyclohexane at 298 K.

in Table 2. **1a** and **1b** exhibited a fluorescence emission around 400 nm, while **1c** showed very weak emission probably on account of the heavy atom effect. Reflecting the red-shift of the UV/Vis absorption maxima, the emission maxima of dibenzochalcogenaborins were also red-shifted on going from **1a** to **1c**. In each case, Stokes shifts were very small ($\Delta E < 2300$ cm^{-1}), indicating the high rigidity of framework of dibenzochalcogenaborins. The concentration effect upon the emission maxima of **1a–c** was not observed. On the other hand, the polarity of the solvent slightly affected the emission maxima. The emission maxima of **1a–c** in dichloromethane ($\varepsilon = 8.93$) are red-shifted compared to those in cyclohexane ($\varepsilon = 2.02$) (λ_{em} in dichloromethane; **1a** 385 nm, **1b** 416 nm, **1c** 430 nm), although absorption maxima of **1a–c** did not shift upon changing the solvent to dichloromethane. These results indicate that the excited states of **1a–c** are slightly polar.

The solid state fluorescence spectra of powder samples of dibenzochalcogenaborins were also measured. **1a** and **1b** showed intense photo-luminescence in the solid state as well as in solution, while **1c** was almost non-emissive in the solid state. The spectra of **1a** and **1b** are shown in Figure 5. Their photophysical data are summarized in Table 3. Intense fluorescence of **1a** and **1b** is observed in the solid state, probably because the sterically bulky Mes group prohibits aggregation, which results in degradation from the excited state through a non-radiative process. The solid-state emissions are red-shifted compared to those in solution, as observed in azaborine, thiaborin, and their ladder-type congeners.[9] These phenomena indicate the existence of dipole–dipole in-
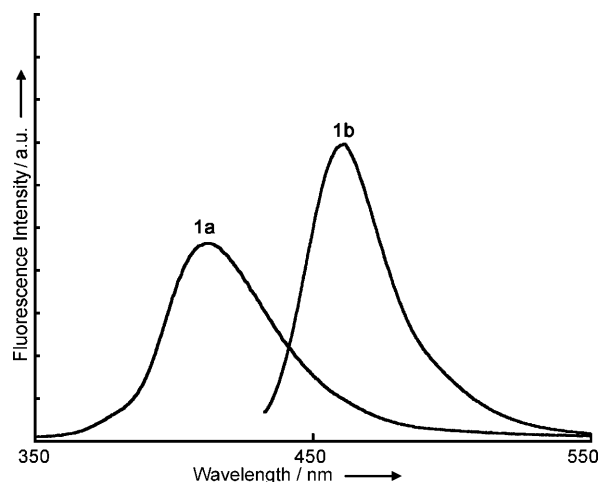

Figure 5. Solid-state fluorescence spectra of chalcogenaborins **1a–c** at 298 K (powder sample)

Table 3. Optical data of chalcogenaborins **1a** and **1b** in the solid state.

compound	λ_{em} [nm][a]	λ_{ex} [nm][b]	ΔE [cm^{-1}][c]
1a	413	378	2.2×10^3
1b	461	430	1.6×10^3

[a] Emission maxima of fluorescence spectra in the solid state. [b] Excitation spectral maxima in the solid state. [c] $\Delta E = 1/\lambda_{ex} - 1/\lambda_{em}$.

teractions in the excited states. Although direct π–π stacking is not significant, as observed in the packing structure of **1a** and **1b**, it is likely that the long-range interaction between excited dipoles may influence the fluorescence emission in the solid state.

Theoretical Calculations

To evaluate the energy levels of molecular orbitals of dibenzochalcogenaborins, theoretical calculations were performed using density functional theory[11] with the model compounds **1a′–c′**, in which the mesityl group is replaced by a phenyl group to reduce the computational time, as well as the methylene bridged analog **1d′** for comparison. The geometry optimizations at B3LYP/6-31+G(d) level reproduced X-ray crystallographic structures of **1a**, **1b** and **1c**. The energy levels of HOMO, HOMO-1, LUMO, and the HOMO–LUMO energy gaps, obtained at B3LYP/6-311+G-(d,p)//B3LYP/6-31+G(d) level, are summarized in Table 4. Orbital plots for the HOMO, HOMO-1, and LUMO of each

Table 4. Frontier molecular orbitals of dibenzochalcogenaborins **1a′–c′** and related compound **1d′**.[a]

compound	HOMO [eV]	LUMO [eV]	HOMO-1 [eV]	ΔE [eV][b]
1a′	−5.65	−1.51	−5.80	4.14
1b′	−5.45	−1.63	−5.86	3.82
1c′	−5.38	−1.69	−5.86	3.69
1d′	−5.61	−1.59	−5.87	4.29

[a] Calculation level: B3LYP/6-311+G(d,p)//B3LYP/6-31+G(d). [b] The energy gap between HOMO and LUMO.

compound are shown in Figure 6. The HOMO of each compound consists of the lone pair orbital of the chalcogen atoms and the π-orbitals on benzene rings. In the case of
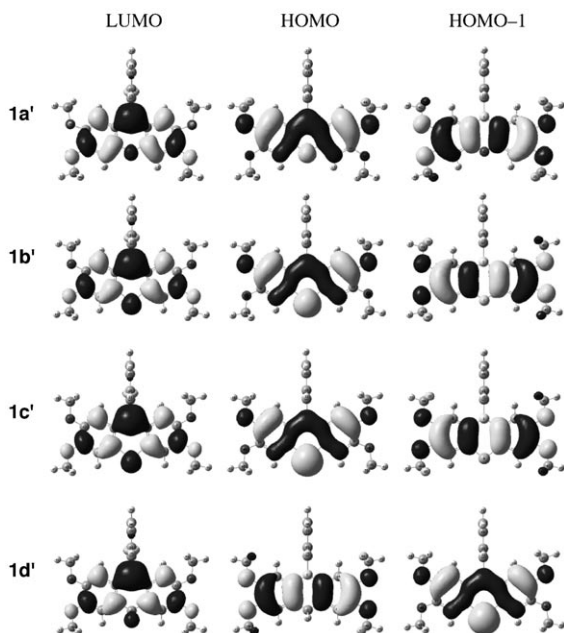

Figure 6. Orbital plots of LUMO, HOMO, and HOMO-1 of dibenzochalcogenaborins **1a′-c′** and the reference compound **1d′**.

1d′, this orbital corresponded to HOMO-1. The energy level of this orbital (HOMO for **1a′**, **1b′**, and **1c′**; HOMO-1 for **1d′**) is elevated in the order of **1d′**, **1a′**, **1b′**, and **1c′**. The elevation of the HOMO energy level in the dibenzochalcogenaborins is consistent with the high energy level of the lone pair orbital of heavier chalcogen atoms. On the other hand, the LUMO energy level decreases from **1a′** to **1c′** and the LUMO energy level of **1b′** and **1c′** is even lower than that of **1d′**. The HOMO-1 consists mainly of π-orbitals on the benzene rings and is rarely affected by changing the bridging chalcogen atoms. A similar behavior, as found for the HOMO and HOMO-1 energy levels of dibenzochalcogenaborins, was observed for the difference of the HOMO and HOMO-1 energy levels of dibenzochalcogenophenes (dibenzofuran, dibenzothiophene, dibenzoselenophene, and dibenzotellurophene).[12]

Time-dependent density functional calculations were also performed to elucidate the transition observed in the UV/Vis spectra. TD-DFT calculations were carried out at B3LYP/6-311+G(d,p)//B3LYP/6-31+G(d) level and the results are summarized in Table 5. Predicted wavelengths matched well with the absorption bands observed in the UV/Vis spectra. The lowest excited state in each compound is contributed by the transition from HOMO to LUMO, that is, intramolecular charge transfer from the lone pair of the chalcogen atom to the vacant orbital of the boron atom. Transition energy is lowered from **1a′** to **1c′** in accordance with the observation in the UV/Vis spectra. The second

Table 5. Time-dependent density functional theory calculations of dibenzochalcogenaborins **1a′–c′**.[a]

compound	E [eV][b]	λ [nm][c]	f[d]	transition
1a′	3.63	341.1	0.0696	HOMO→LUMO
	3.87	320.6	0.3672	HOMO-1→LUMO
1b′	3.33	372.1	0.0744	HOMO→LUMO
	3.17	329.0	0.2306	HOMO-1→LUMO
1c′	3.20	387.6	0.0791	HOMO→LUMO
	3.70	335.4	0.2213	HOMO-1→LUMO

[a] Calculation level: B3LYP/6-311+G(d,p)//B3LYP/6-31+G(d). [b] Excitation energy. [c] Wavelength. [d] Oscillator strength.

lowest excited state is attributed to the transition form HOMO-1 to LUMO, and does not show a large difference among chalcogen congeners.

Conclusions

In this study, we synthesized dibenzochalcogenaborins and compared their structural and optical properties systematically. These molecules were shown to have a rigid and planar framework, as determined from X-ray crystallographic analysis and theoretical calculations. UV/Vis and fluorescence spectroscopy as well as theoretical calculations, proved that the nature of chalcogen atoms at the bridging position strongly affects their optical and electronic properties. Dibenzooxaborin and dibenzothiaborin emitted intense fluorescence both in solution and in the solid state because of the rigid framework and inhibition of strong intermolecular interactions like π–π stacking in the solid state, while dibenzoselenaborin showed only weak fluorescence in solution. The HOMO–LUMO energy gap was found to decrease on going down the periodic table for the choice of bridging chalcogen atoms.

Experimental Section

General Procedure

General chemicals were used as received. Cyclohexane and THF, spectrochemical or fluorometric grade (Dojindo), were used for optical measurement. All manipulations were carried out using modified Schlenk technique under an argon atmosphere. Solvents were purified by MBRAUN MB-SPS system. Wet column chromatography (WCC) was performed using Kanto Silica Gel 60N. Gel permeation liquid chromatography (GPC) was performed using LC-918 with JAIGEL 1H+2H columns (Japan Analytical Industry) using chloroform as solvent. NMR spectra were recorded by a Bruker DRX-500 spectrometer (^{1}H, 500 MHz; ^{13}C, 126 MHz) and a JEOL AL-400 spectrometer (^{11}B, 128 MHz). Chemical shifts δ are reported in ppm. ^{1}H NMR spectra are referenced to residual protons in the deuterated solvent; ^{13}C NMR spectra are referenced to carbon-13 in the deuterated solvent; ^{11}B NMR spectra are referenced to an external standard of BF₃·Et₂O. UV/Vis spectra were recorded on a JASCO V-530 spectrophotometer. Fluorescence spectra were recorded on a JASCO F-6500 fluorescence spectrophotometer. All melting points were measured with a Yanaco MP-S3 and were uncorrected. Elemental analyses were performed by the Microanalytical Laboratory of the Department of Chemistry, Faculty of Science, The University of Tokyo. Bis(2-bromo-4,5-dimethoxyphenyl) ether **2a**, bis(2-bromo-

4,5-dimethoxyphenyl) sulfide **2b**, and bis(2-bromo-4,5-dimethoxyphenyl) selenide **2c** were prepared according to the literature.[10]

Synthesis

1a: 9-Mesityl-9*H*-9-boraxanthene. *t*BuLi (2.2 M pentane solution, 6.1 mL, 13.4 mmol) was added to a solution of bis(2-bromo-4,5-dimethoxyphenyl) ether **2a** (1.37 g, 3.06 mmol) in THF (30 mL) at −78 °C. After stirring for 30 min at −78 °C, MesB(OMe)$_2$ (824.5 mg, 4.29 mmol) was added to the reaction mixture at −78 °C. The reaction mixture was refluxed overnight and the reaction was quenched with water. The organic layer was extracted with CHCl$_3$ and the extracts were combined and dried over anhydrous MgSO$_4$. After removal of the solvent under reduced pressure, the residue was purified by reprecipitation from CHCl$_3$/MeOH to give **1a** as a pale yellow solid (493.6 mg, 39%). m.p. 224–225 °C; ^{1}H NMR (500 MHz, CDCl$_3$, r.t.): $\delta = 7.25$ (s, 2H), 6.94 (s, 2H), 6.91 (s, 2H), 4.01 (s, 6H), 3.77 (s, 6H), 2.38 (s, 3H), 2.00 ppm (s, 6H); ^{13}C NMR (126 MHz, CDCl$_3$, r.t.): $\delta = 155.4$, 154.6, 145.2, 138.8, 138.0, 136.5, 127.0, 117.4, 114.2, 99.6, 56.3, 56.1, 22.7, 21.3 ppm; ^{11}B NMR (128 MHz, CDCl$_3$, r.t.): $\delta = 52$ ppm; UV/Vis (cyclohexane): λ_{max} (ε) = 347 (sh, 11000), 320 (22000); elemental analysis calcd (%) for C$_{25}$H$_{27}$BO$_5$: C 71.78, H 6.51; found: C 71.51, H 6.65.

1b: 9-Mesityl-9*H*-9-borathioxanthene. *t*BuLi (2.2 M pentane solution, 4.0 mL, 8.8 mmol) was added to a solution of bis(2-bromo-4,5-dimethoxyphenyl) sulfide **2b** (0.93 g, 2.02 mmol) in Et$_2$O (30 mL) at −78 °C. After stirring for 30 min at −78 °C, MesB(OMe)$_2$ (535.8 mg, 2.79 mmol) was added to the reaction mixture at −78 °C. The reaction mixture was refluxed overnight and the reaction was quenched with water. The organic layer was extracted with CHCl$_3$, and the extracts were combined and dried over anhydrous MgSO$_4$. After removal of the solvent under reduced pressure, the residue was subjected to silica gel column chromatography (CHCl$_3$/nHex = 2:1) and GPC to give **1b** as a pale yellow solid (276.0 mg, 23%). m.p. 229 °C; ^{1}H NMR (500 MHz, CDCl$_3$, RT): $\delta = 7.18$ (s, 2H), 7.17 (s, 2H), 6.89 (s, 2H), 4.00 (s, 6H), 3.71 (s, 6H), 2.37 (s, 3H), 1.94 ppm (s, 6H); ^{13}C NMR (126 MHz, CDCl$_3$, RT): $\delta = 152.7$, 146.9, 138.5, 138.0, 137.3, 136.3, 127.2, 126.9, 119.0, 106.5, 56.0, 56.0, 22.3, 21.3 ppm; ^{11}B NMR (128 MHz, CDCl$_3$, RT): $\delta = 54$ ppm; UV/Vis (cyclohexane): λ_{max} (ε) = 382 (7100), 326 (15000); elemental analysis calcd (%) for C$_{25}$H$_{27}$BO$_4$S: C 69.13, H 6.27; found: C 68.88, H 6.28.

1c: 9-Mesityl-9*H*-9-bora-10-selenaanthracene. *t*BuLi (2.2 M pentane solution, 2.8 mL, 6.1 mmol) was added to a solution of bis(2-bromo-4,5-dimethoxyphenyl) selenide **2c** (0.70 g, 1.38 mmol) in Et$_2$O (30 mL) at −78 °C. After stirring for 30 min at −78 °C, MesB(OMe)$_2$ (370.7 mg, 1.93 mmol) was added to the reaction mixture at −78 °C. The reaction mixture was refluxed overnight and the reaction was quenched with water. The organic layer was extracted with CHCl$_3$, and the extracts were combined and dried over anhydrous MgSO$_4$. After removal of the solvent under reduced pressure, the residue was subjected to silica gel column chromatography (CHCl$_3$) and GPC to give **1c** as a yellow solid (156.0 mg, 24%). m.p. 188 °C; ^{1}H NMR (500 MHz, CD$_2$Cl$_2$, RT): $\delta = 7.28$ (s, 2H), 7.21 (s, 2H), 6.90 (s, 2H), 3.95 (s, 6H), 3.62 (s, 6H), 2.36 (s, 3H), 1.91 ppm (s, 6H); ^{13}C NMR (126 MHz, CDCl$_3$, RT): $\delta = 152.6$, 147.1, 141.4, 138.3, 137.4, 136.3, 128.9, 126.9, 121.1, 108.8, 56.0, 55.9, 22.6, 21.3 ppm; ^{11}B NMR (128 MHz, CDCl$_3$, RT): $\delta = 57$ ppm; UV/Vis (cyclohexane): λ_{max} (ε) = 392 (7100), 331 (16000); elemental analysis calcd (%) for C$_{25}$H$_{27}$BO$_4$Se: C 62.30, H 5.65; found: C 62.28, H 5.70.

X-ray Crystallography

1a, 1b, and 1c: Crystallographic data for **1a**: C$_{25}$H$_{27}$BO$_4$·C$_2$H$_3$N, pale yellow block, monoclinic, space group $C2/c$, $a = 36.365(13)$ Å, $b = 23.334(8)$ Å, $c = 8.268(3)$ Å, $\beta = 102.7605(14)°$, $V = 6842(4)$ Å^3, $Z = 12$, $F(000) = 2964$, crystal size $0.40 \times 0.40 \times 0.30$ mm^3, $6.14 \leq 2\Theta \leq 50.00$. In total, 21596 reflections were collected, of which 5975 were independent ($R_{int} = 0.0227$) and employed for refinement: 450 parameters, 0 restraints, Goodness of fit on $F^2 = 1.050$, R_1 ($I > 2\sigma(I)$) = 0.0518, wR_2 (all data) = 0.1588. Crystallographic data for **1b**: C$_{25}$H$_{27}$BSO$_4$, pale yellow block, monoclinic, space group $P\bar{1}$, $a = 7.941(4)$ Å, $b = 13.192(7)$ Å, $c = 22.448(12)$ Å, $\alpha = 95.987°$, $\beta = 90.598(7)°$, $\gamma = 103.874(8)°$, $V = 2269(2)$ Å^3, $Z = 4$, $F(000) = 920$, crystal size $0.20 \times 0.20 \times 0.20$ mm^3, $6.04 \leq 2\Theta \leq 50.00$. In total, 14375

reflections were collected, of which 7741 were independent ($R_{int} = 0.0451$) and employed for refinement: 721 parameters, 0 restraints, Goodness of fit on $F^2 = 0.969$, R_1 ($I > 2\sigma(I)$) = 0.0534, wR_2 (all data) = 0.1437. Crystallographic data for **1c**: C$_{25}$H$_{27}$BSeO$_4$·CHCl$_3$, yellow block, monoclinic, space group $P2_1/n$, $a = 17.2958(17)$ Å, $b = 8.0957(5)$ Å, $c = 20.0850(15)$ Å, $\beta = 98.1777(11)°$, $V = 2783.7(4)$ Å^3, $Z = 4$, $F(000) = 1224$, crystal size $0.20 \times 0.20 \times 0.20$ mm^3, $6.04 \leq 2\Theta \leq 50.00$. In total, 16917 reflections were collected, of which 4829 were independent ($R_{int} = 0.0410$) and employed for refinement: 360 parameters, 0 restraints, Goodness of fit on $F^2 = 1.021$, R_1 ($I > 2\sigma(I)$) = 0.0369, wR_2 (all data) = 0.0951. The intensities of reflections were collected at 120 K on a RIGAKU MSC Mercury CCD diffractometer with graphite-monochromated Mo$_{K\alpha}$ radiation ($\lambda = 0.71070$ Å) using CrystalClear (Rigaku Corp.). The structure was solved by direct methods (SHELXS) and expanded using Fourier techniques. The structure was refined by full-matrix least-squares methods on F^2 (SHELXL-97).[13] All non-hydrogen atoms were refined anisotropically. Hydrogen atoms were assigned idealized positions and were included in structure factor calculations. CCDC 667887, CCDC 667888 and CCDC 667889 contain the supplementary crystallographic data for **1a**, **1b** and **1c**, respectively. These data can be obtained free of charge from the Cambridge Crystallographic Data Centre at www.ccdc.cam.ac.uk/conts/retrieving.html (or from the Cambridge Crystallographic Data Centre, 12, Union Road, Cambridge CB21EZ, UK; fax: (+44) 1223–336–033; or deposit@ccdc.cam.ac.uk).

[1] a) S. Yamaguchi, K. Tamao, *Chem. Lett.* **2005**, *34*, 2; b) M. Hissler, P. W. Dyer, R. Réau, *Top. Curr. Chem.* **2005**, *250*, 127.

[2] a) U. Salzner, J. B. Lagowski, P. G. Pickup, R. A. Poirier, *Synth. Met.* **1998**, *96*, 177; b) S. Yamaguchi, K. Tamao in *The Chemistry of Organic Silicon Compounds, Vol. 3* (Eds.: Z. Rappoport, Y. Apeloig), Wiley, Chichester, **2001**, pp. 641–694; c) S. Yamaguchi, K. Tamao, *J. Organomet. Chem.* **2002**, *653*, 223; d) S. Yamaguchi, K. Tamao, *J. Organomet. Chem.* **2000**, *611*, 5; e) S. Yamaguchi, T. Endo, M. Uchida, T. Izumizawa, K. Furukawa, K. Tamao, *Chem. Eur. J.* **2000**, *6*, 1683; f) M. Hissler, P. W. Dyer, R. Réau, *Coord. Chem. Rev.* **2003**, *244*, 1; g) M. G. Hobbs, T. Baumgartner, *Eur. J. Inorg. Chem.* **2007**, 3611; h) T. Baumgartner, R. Réau, *Chem. Rev.* **2006**, *106*, 4681; i) A. Fukazawa, M. Hara, T. Okamoto, E.-C. Son, C. Xu, K. Tamao, S. Yamaguchi, *Org. Lett.* **2008**, *10*, 913.

[3] a) C. D. Entwistle, T. B. Marder, *Chem. Mater.* **2004**, *16*, 4574; b) S. Yamaguchi, A. Wakamiya, *Pure Appl. Chem.* **2006**, *78*, 1413.

[4] a) P. M. Maitlis, *J. Chem. Soc.* **1964**, 425; b) M. Kranz, F. Hampel, T. Clark, *J. Chem. Soc. Chem. Commun.* **1992**, 1247; c) M. B. Ryzhikov, A. N. Rodionov, V. V. Nekrasov, D. N. Shigorin, *Zh. Fiz. Khim.* **1988**, *62*, 2491; d) M. B. Ryzhikov, A. N. Rodionov, O. V. Nesterova, D. N. Shigorin, *Zh. Fiz. Khim.* **1998**, *62*, 1067.

[5] a) M. V. Metz, D. J. Schwartz, C. L. Stern, P. N. Nickias, T. J. Marks, *Angew. Chem.* **2000**, *112*, 1368; *Angew. Chem. Int. Ed.* **2000**, *39*, 1312; b) V. C. Williams, C. Dai, Z. Li, S. Collins, W. E. Piers, W. Clegg, M. R. J. Elsegood, T. B. Marder, *Angew. Chem.* **1999**, *111*, 3922; *Angew. Chem. Int. Ed.* **1999**, *38*, 3695; c) P. Mueller, S. Huck, H. Koeppel, H. Pritzkow, W. Siebert, *Z. Naturforsch. B* **1995**, *50*, 1476; d) H. Schulz, H. Pritzkow, W. Siebert, *Chem. Ber.* **1991**, *124*, 2203.

[6] M. Melaïmi, S. Sóle, C.-W. Chiu, H. Wang, F. P. Gabbaï, *Inorg. Chem.* **2006**, *45*, 8136.

[7] S. Sóle, F. P. Gabbaï, *Chem. Commun.* **2004**, 1284.

[8] a) T. Agou, J. Kobayashi, T. Kawashima, *Org. Lett.* **2005**, *7*, 4373; b) T. Agou, J. Kobayashi, T. Kawashima, *Inorg. Chem.* **2006**, *45*, 9137; c) M. H. Lee, T. Agou, J. Kobayashi, T. Kawashima, F. P.

Gabbaï, *Chem. Commun.* **2007**, 1133; d) T. Agou, J. Kobayashi, Y. Kim, F. P. Gabbaï, T. Kawashima, *Chem. Lett.* **2007**, *36*, 976.

[9] a) T. Agou, J. Kobayashi, T. Kawashima, *Org. Lett.* **2006**, *8*, 241; b) T. Agou, J. Kobayashi, T. Kawashima, *Chem. Eur. J.* **2007**, *13*, 8051; c) T. Agou, J. Kobayashi, T. Kawashima, *Chem. Commun.* **2007**, 3204.

[10] L. Engman, J. Hellberg, C. Ishag, *J. Chem. Soc. Perkin Trans. 1* **1988**, 2095.

[11] *Gaussian 03*, Revision C.02, M. J. Frisch, G. W. Trucks, H. B. Schlegel, G. E. Scuseria, M. A. Robb, J. R. Cheeseman, J. A. Montgomery, Montgomery, Jr., T. Vreven, K. N. Kudin, J. C. Burant, J. M. Millam, S. S. Iyengar, J. Tomasi, V. Barone, B. Mennucci, M. Cossi, G. Scalmani, N. Rega, G. A. Petersson, H. Nakatsuji, M. Hada, M. Ehara, K. Toyota, R. Fukuda, J. Hasegawa, M. Ishida, T. Nakajima, Y. Honda, O. Kitao, H. Nakai, M. Klene, X. Li, J. E. Knox, H. P. Hratchian, J. B. Cross, V. Bakken, C. Adamo, J. Jaramillo, R. Gomperts, R. E. Stratmann, O. Yazyev, A. J. Austin, R. Cammi, C. Po-

melli, J. W. Ochterski, P. Y. Ayala, K. Morokuma, G. A. Voth, P. Salvador, J. J. Dannenberg, V. G. Zakrzewski, S. Dapprich, A. D. Daniels, M. C. Strain, O. Farkas, D. K. Malick, A. D. Rabuck, K. Raghavachari, J. B. Foresman, J. V. Ortiz, Q. Cui, A. G. Baboul, S. Clifford, J. Cioslowski, B. B. Stefanov, G. Liu, A. Liashenko, P. Piskorz, I. Komaromi, R. L. Martin, D. J. Fox, T. Keith, M. A. Al-Laham, C. Y. Peng, A. Nanayakkara, M. Challacombe, P. M. W. Gill, B. Johnson, W. Chen, M. W. Wong, C. Gonzalez, J. A. Pople, Gaussian, Inc., Wallingford CT, **2004**.

[12] O. G. Rodin, V. V. Redchenko, A. B. Kostitsyn, V. F. Traven, *Zh. Obshch. Khim.* **1988**, *58*, 1409.

[13] G. M. Sheldrick, SHELXL-97, Program for Crystal Structure Refinement, University of Göttingen, Göttingen (Germany), **1997**.